

High-power Kerr-lens mode-locked thin-disk oscillator in the anomalous and normal dispersion regimes

Oleg Pronin^a, Jonathan Brons^b, Marcus Seidel^b, Fabian Lücking^a, Christian Grasse^c, Gerhard Boehm^c, Markus C. Amann^c, Vladimir Pervak^b, Alexander Apolonski^{ab}, Vladimir L. Kalashnikov^d and Ferenc Krausz^{ab}

^aLudwig-Maximilians-Universität München, Germany;

^bMax-Planck-Institut für Quantenoptik, Garching, Germany

^cWalter Schottky Institut, Garching, Germany

^dInstitut für Photonik, TU Wien, Vienna, Austria

ABSTRACT

A femtosecond thin-disk Yb:YAG oscillator in both the anomalous and the normal dispersion regime is demonstrated. Both regimes are realized with practically the same resonator configuration. The power scaling potential of the anomalous and normal dispersion regimes is analyzed both theoretically and experimentally. The recipe to obtain Kerr-lens mode-locking (KLM) in the thin-disk configuration is presented here and oscillator characteristics as well as start-up difficulties are described. The oscillator stability in terms of output power, beam pointing and sensitivity to back reflections is measured and corresponds to the level of commercial systems.

Keywords: (140.3480) Lasers, diode-pumped; (140.3580) Lasers, solid-state; (140.4050) Mode-locked lasers

1. INTRODUCTION

High-harmonic generation (HHG) at MHz repetition rate is one of the particularly interesting topics leading to the large range of the applications. Due to the very low conversion efficiency (10^{-8} - 10^{-6}) of the HHG process¹ and the low average power amplifier systems driving at kHz repetition rate, the resulting average XUV power is well below the mW level. This fact restricts the field of HHG applications. Attosecond pulse generation,¹ high-resolution spectroscopy with XUV frequency combs,^{2,3} pump-probe measurements, photoelectron emission microscopy, photoelectron imaging spectroscopy, pump-probe diffraction experiments with electrons and nanostructure characterization could substantially benefit from MHz-repetition-rate XUV sources. For many of these experiments the output of the signal level is very low and data acquisition over many hours or days is necessary when operated at \sim kHz repetition rate. A difference of three to four orders can be gained by working at MHz repetition rate. Experiments such as electron diffraction⁴ with fs time resolution can be enabled only in the single electron regime (because of the space charge) and ultimately need MHz laser sources.

One of the approaches is to use a passive femtosecond enhancement resonator^{2,5} for storage of radiation. By using this method, one can increase the power from a mode-locked seed oscillator by a large factor (10 - 10^4) inside the cavity. Extremely low-loss optics and fine dispersion control of the cavity are needed. Moreover, the cavity has to be kept in resonance with the seeding oscillator and mode-matched to it. Nevertheless, due to the low XUV conversion efficiency an enhancement cavity recycles circulating pulses with rather small influence on the enhancement factor and remains the most promising tool in accessing HHG at MHz repetition rate.

The idea of utilizing the high average powers inside a laser oscillator cavity has become a reality with recent progress in high-power femtosecond thin-disk (TD) lasers.⁶⁻⁸ Typically, the output coupler transmission T of an oscillator amounts to only a few per cent. This means that power stored inside the oscillator cavity is a factor $\sim 1/T$ higher than the output power. On the other hand, the oscillator is a dynamic nonlinear system which cannot simply be operated at arbitrarily high energies due to the instabilities of mode-locking. Recently, the first

Further author information: (Send correspondence to Oleg Pronin)
Oleg Pronin: oleg.pronin@mpq.mpg.de, Telephone: +498928914637

proof of principle experiment on laser intracavity HHG was demonstrated in Ref.⁹ with Ti:Sa bulk oscillator having 17 fs, 1 μ J pulses intracavity.

For any of the approaches (amplifier system, enhancement cavity, laser intracavity) the oscillator continues to be the decisive element. An energy-upscaled seed oscillator ($>\mu$ J) can eliminate the need for pre-amplification stages and thus simplify the system. A lesser gain needed from the amplifier results in less gain narrowing and shorter pulses after compression can be realized. The enhancement cavity combined with a high-energy table-top compact oscillator becomes an attractive tool for XUV generation in many labs. The constraints on the enhancement factor can be substantially lowered when seed oscillators with higher pulse energies become available. Progress on the development of a Kerr-lens thin-disk oscillator allows intra-cavity peak intensities similar to those of the first generation of enhancement cavities.²

In contrast to TD oscillators, bulk oscillators are not power-scalable and their pulse-energies can only be increased by lowering the repetition rate. Thus the development of Ti:Sa oscillators culminated in the output pulse energies of >500 nJ¹⁰ and more recently >650 nJ in commercial systems¹¹ with 50-fs pulse duration. Ti:Sa oscillators generating sub-10 fs¹² and even sub-6 fs¹³ with several nJ pulse energies were developed. The average power of Ti:Sa bulk oscillators remains in the range of several watts. Other Yb bulk oscillators with different gain media could approach the level of 10 W.¹⁴ Fibre and innoslab amplifier systems^{15,16} are operating in a way similar to kHz amplifier systems, but at MHz repetition rate and corresponding power levels approaching 1 kW. These systems continue to be fairly complex, bulky and expensive. The power scalability of TD technology makes it a promising candidate for developing the next generation of femtosecond oscillators, yielding average output powers exceeding 140 W,^{6,7} pulse energies of 40 μ J⁶ and pulse durations of 600-1000 fs. Until recently,⁸ all TD oscillators had been mode-locked with semiconductor saturable absorber mirrors (SESAM). Their moderate modulation depth and finite relaxation time prevented the generation of pulses shorter than 600 fs in Yb:YAG. In contrast, nearly gain-bandwidth-limited pulse generation from a TD Yb:YAG oscillator is demonstrated via KLM.⁸ It will be shown further that pulses shorter than 200 fs can be generated even from Yb:YAG and even shorter in other Yb-doped TD oscillators. The many shortcomings originating from SESAM are not intrinsic to the KLM method.

2. KLM OSCILLATOR IN THE ANOMALOUS DISPERSION REGIME

So far, all femtosecond TD oscillators have been mode-locked by means of SESAM. The KLM technique has been proposed many times and simultaneously criticized as difficult to realize.¹⁷⁻¹⁹ Actually, the limitations caused by SESAM* were the most motivating factor for experiments on the KLM TD oscillator. The main concerns and uncertainties in initiating this work were the natural coupling between SPM and self-focusing (the main mechanism for mode-locking), initiation of mode-locking and the influence of the TD thermal lens.

2.1 KLM cavity

The cavity configuration used for most mode-locking experiments is the bow-tie illustrated in Fig.1 or so-called X-shape cavity or Z-shape cavity. These types of resonators were analyzed in detail in.²⁰⁻²³

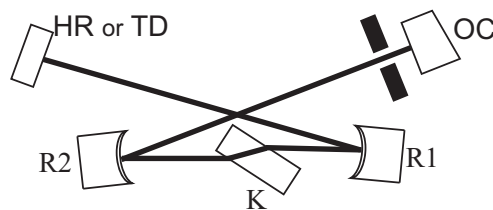


Figure 1. Schematic of the X-shape resonator standardly used for low-power bulk oscillators. *R1*, *R2*, concave mirrors; *K*, Kerr medium; *OC*, output coupler. The replacement of the HR mirror by a TD leads to a design proposed in Ref.²⁴ for KLM realization in a TD oscillator.

*at least, by the SESAMs available from Batop, ANU, Reflekron, WSI

As one can see, the resonator configuration of the TD oscillator in Fig.3 is more complex in relation to that in Fig.1. First, in Fig.1 the Kerr medium simultaneously serves as a gain medium. This is not only hard to realize but also unnecessary in the TD configuration. It would strongly counteract the power-scaling concept, according to which the pump power density should be kept constant by enlarging the mode area on the disk and proportionally increasing the pump power. Moreover, the disk is too thin to exhibit reasonable self-focusing. There are a number of publications in which the gain medium and Kerr medium were separated. These are the experiments on Kerr-lens mode-locking of Nd:YAG²⁵ and Nd:YLF²⁶ lasers. Indeed, they also have bow-tie-type cavities. This type of cavity is not used in the TD configuration because of the small mode diameters over the optical elements, which is typically below 1 mm. The simple and convenient solution for KLM in the TD cavity was to implement a telescopic arrangement inside the cavity, which, in first approximation, can be considered as a 4f extension. This resonator configuration shows average mode diameters >2 mm over the intracavity optical elements.

2.2 Starting the KLM

One of the few drawbacks accompanying KLM is the difficult initiation of mode-locking. Small random initial intensity fluctuations are too weak to make the self-focusing effect pronounced. Thus, external cavity perturbation is necessary to induce stronger fluctuations and initiate pulse build-up. It can be accomplished by i) moving one of the cavity mirrors or ii) placing one of the mirrors on a piezo transducer or shaker,²⁷ or iii) by using active mode-locking,^{26,28} iv) semiconductor-doped glass structures²⁹ or v) SESAM¹³ for initial pulse build-up. In any case the oscillator has to operate near the stability edge where the oscillator is most susceptible to intensity fluctuations. This is typically accomplished by changing the distance between two focusing mirrors. In Fig.2 the

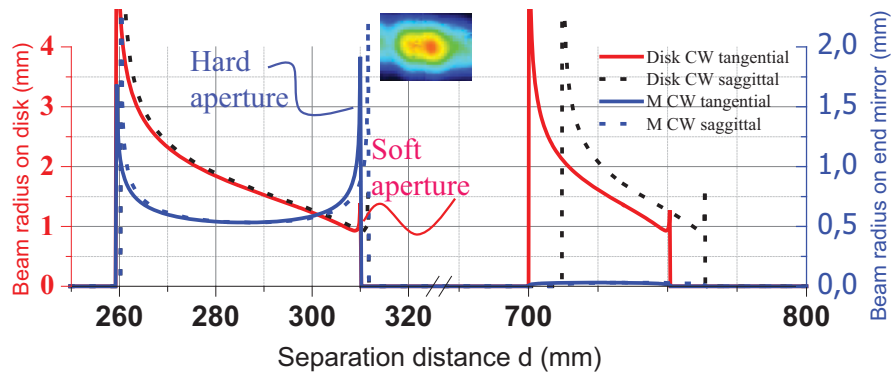


Figure 2. Mode sizes on the disk and end mirror vs separation distance d for the CW cavity. The inset shows a strongly astigmatic beam profile at the stability edge corresponding to $d \sim 312$ mm.

CW behaviour of the resonator at different stability edges is shown. Four stability edges appear as a function of the separation distance d . The stability edge corresponding to $d \sim 312$ mm was used in this work. The inset shows a strongly astigmatic CW beam profile at the stability edge which agrees well with calculations. In principle, measurements of the beam profile at different cavity mirrors can be performed to derive the position with respect to the stability edge in the KLM regime.

In some respect the starting problem is similar to the situation described for the SESAM mode-locked case³⁰ when the mode-locker cannot be optimized for a whole range of energies and peak powers. Some weak mode-locking mechanism is needed to cover the low-energy range and pass on the baton to KLM for higher peak powers. Indeed, the situation concerning start-up is not very critical and is a subject for optimization. For example, self-starting stably mode-locked pure-KLM oscillators were demonstrated,²¹ and even turn-key commercial stable self-starting systems with <10 fs pulse duration are available.¹¹ It is worth noting that such an oscillator experiences a peak-power change of six to seven orders of magnitude.

2.2.1 Weak SESAM

SESAM used to be the intracavity element most susceptible to damage in high-power systems, typically via self-Q-switching or relaxation oscillation spikes during the pulse buildup process. Moreover, it also exhibits two-

photon absorption (TPA), which tends to give rise to breakup into multi-pulsing and limits both the achievable intracavity pulse energy and minimum pulse duration. However, the use of a SESAM as a starter for mode-locking strongly reduces constraints on the cavity design. In that case, it is no longer necessary to keep the saturable absorption large and relaxation time very short to maintain mode-locking. These considerations inspired us to design a SESAM more suitable to start mode-locking. We applied a dielectric top coating on a one quantum-well (InGaAs) SESAM. The top reflective dielectric coating consists of six alternating layers of Ta_2O_5 (128 nm) and SiO_2 (178 nm). The coating reduces the intensity level in the SESAM by a factor of 9. As a consequence, the SESAM modulation depth drops by the same factor to $\Delta R < 0.1\%$ and the saturation fluence rises to $F_{sat} > 400 \mu\text{J}/\text{cm}^2$, which leads to reduced TPA and an increased damage threshold.³¹ Because of the small modulation depth, this SESAM alone cannot result in stable mode-locking. To our knowledge, such a low-modulation-depth weak SESAM was used as KLM starter for the first time.

In the experiments described below we used an OC with transmission of 5.5% and a weak SESAM as end mirror M. The experiment with OC transmission of 14% and HR as end mirror will be treated separately.

As a first approximation we took the Kerr-lens as a thin lens and used simple ABCD calculations to model the influence of the Kerr-lens. Such simulations gave a qualitative understanding of the cavity behaviour at the stability edge and possible influence of the Kerr lens on it.

3. KERR-LENS MODE-LOCKING OF YB:YAG OSCILLATOR

Kerr-lens mode-locking of an Yb:YAG bulk oscillator was already performed by S. Uemura et al. and resulted in 35-fs pulses.³² This remarkable performance came at the expense of dramatically reduced output power and efficiency, achieved by spectral filtering which shifted the central wavelength from 1030 nm toward 1060 nm, limiting the output power to 110 mW. Even so, this can be compared with results for a similar bulk oscillator configuration mode-locked by a SESAM. In this case the shortest pulses were about 340 fs and the output power 110 mW.³³

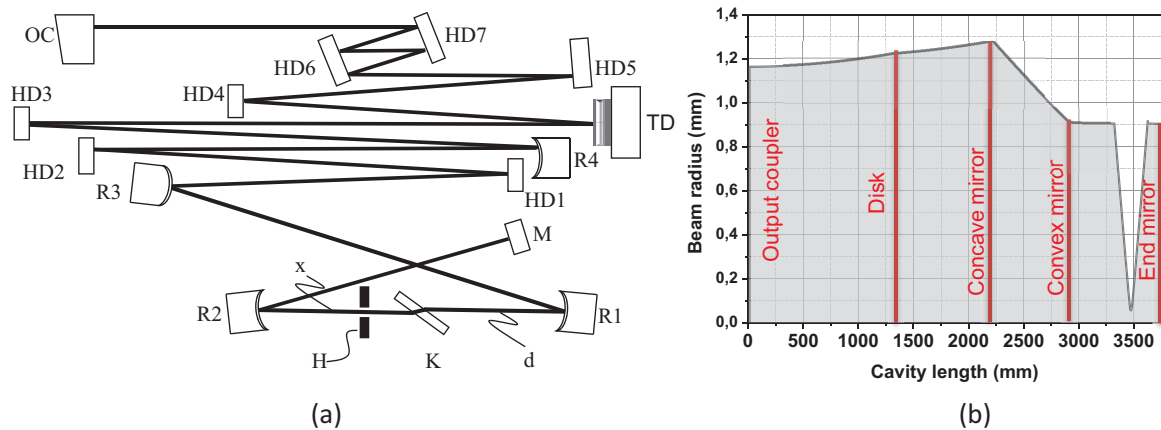


Figure 3. (a): Schematic of the KLM Yb:YAG disk oscillator in the presence of anomalous GDD. All flat mirrors are HD mirrors with $\beta = -1000 \text{ fs}^2$ and $\beta = -3000 \text{ fs}^2$ per bounce; OC, an output coupler with 5.5% or 14% transmission; $R1, R2$ concave mirrors with 0.3 m radius of curvature ; $R3 = -4 \text{ m}$; $R4 = 4 \text{ m}$; K , Kerr medium; H , hard aperture; M , weak SESAM or HR mirror. The pulse repetition rate is 40 MHz. (b): Mode radius vs cavity length. Calculated for the concave TD with $R_{TD} = 25 \text{ m}$.

Our experimental setup, sketched in Fig.3, includes a 220- μm thin-wedged Yb:YAG disk of 7% doping from D+G GmbH. A disk head is aligned for 24 passes of the pump beam through the gain medium with a pump spot diameter of 3.2 mm. The Yb:YAG TD is used as one of the folding mirrors in a standing-wave cavity pumped by fibre-coupled diodes centred at a wavelength of 940 nm. The cavity is a convex–concave type designed for providing large mode sizes over its entire length, in order to minimize nonlinear propagation effects in air and also the risk of damage to optical components. As we can see in Fig.3, the average mode radius inside the cavity

is >1 mm, and the beam radius on the disk is ~ 1.2 mm and 0.9 mm on the end mirror M . Dispersion from all intracavity elements as well as the nonlinear phase shift induced by the Kerr-medium are compensated for by the round-trip negative GDD of approximately -22.000 fs². All flat mirrors were high-dispersive (HD) mirrors with -1000 fs² and -3000 fs² per bounce.³⁴ In order to provide high sensitivity of the Kerr effect, the oscillator is operated at the stability edge corresponding to the increased distance d between mirrors $R1$ and $R2$. This stability edge can be used for both soft- and hard-aperture KLM.

3.1 Experiments with different Kerr media

In the beginning lead-containing SF 57 glass, with a high nonlinear refractive index $n_2=4.1\cdot 10^{-19}$ m²/W was chosen as Kerr medium to enhance the self-focusing effect and identify the resonator configuration and alignment necessary to obtain KLM. Mirror R2 was mounted on a precision micrometer stage. A gradual increase of the distance d resulted in a gradual decrease of the output power and changed the beam profile to more astigmatic. Near the stability edge the output power substantially dropped because of the poor overlap with the pump spot on the TD. This point serves as a reference near which Kerr lensing can be obtained. The mode-locking could

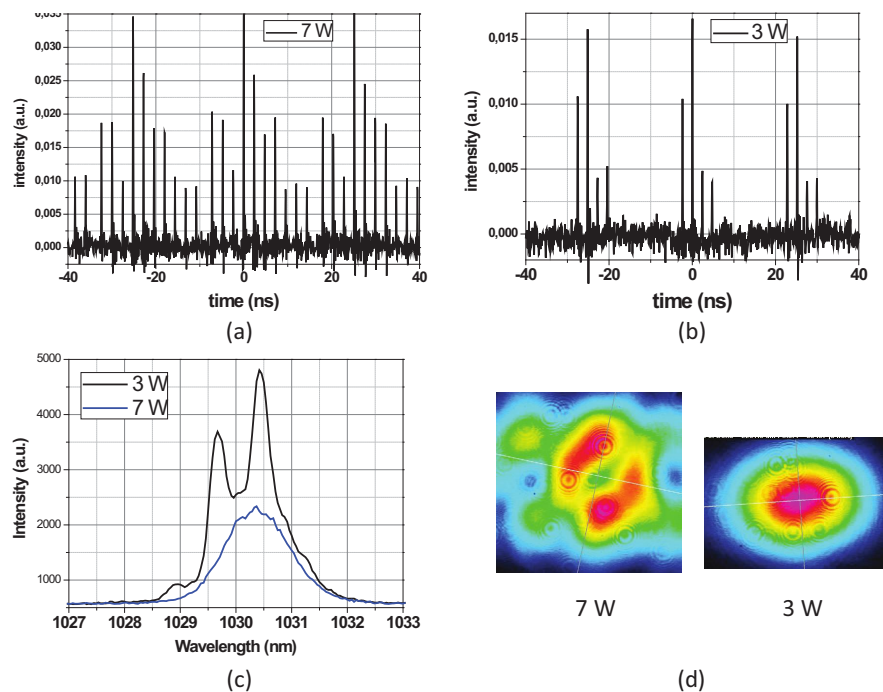


Figure 4. Oscillator characteristics operating with 4-mm-thick SF 57 glass plate as Kerr medium. (a): Pulse train at 7 W output power; (b): Pulse train at 3 W output power; (c): Optical spectra at 3 W and 7 W output power (measured with Ocean Optics HR 4000); (d): Beam profile at 3 W and 7 W output power.

be started by pushing mirror $R2$ and carefully aligning the position of the Kerr medium relative to the focus (distance x in Fig. 3). The latter alignment was not critical because a 4-mm-thick SF 57 plate can be placed in the focus with a small uncertainty. The distance d had to be increased to ≈ 312 mm in order to bring the cavity to the edge of the stability zone. It is clear that the beam radius of $50\text{-}100$ μm in the Kerr medium and the high nonlinearity of SF 57 glass cause very high SPM, which cannot be balanced by the GDD of -22000 fs² introduced in the cavity. Unavoidably, this situation leads to unstable mode-locking with onset of multi-pulsing. Up to 10 pulses per cavity round-trip could be detected with a fast photodiode at 7 W output power and 70 W pump power (see Fig.4(a)). A 5.5% OC was chosen to decrease the lasing threshold and keep the intracavity power relatively large for initial experiments. Decreasing the pump power down to 50 W and 3 W output power reduces the amount of pulses down to 3 (see Fig.4(b)). The spectral bandwidth, however, does not change appreciably and maintains $\Delta\lambda_{FWHM} \approx 1.5$ nm (see Fig.4(c)). Pronounced CW spikes appear at reduced output power. The

thinner 1.8-mm plate of SF 57 glass was tried out as next step. It did not change the situation drastically as strong multi-pulsing and optical spectra with similar bandwidth were observed.

As a next step the 6.4-mm-thick fused silica plate with $n_2=2.5 \cdot 10^{-20} \text{ m}^2/\text{W}^{35}$ was taken. It reduced the nonlinearity by almost an order of magnitude in relation to the 4-mm-thick SF 57 plate and simultaneously kept the plate thick in order to have no constraint on the alignment relatively to the beam focus. This could slightly improve the situation. The optical spectrum became broader with $\Delta\lambda_{FWHM} \approx 3 \text{ nm}$ for the mode-locked regime with onset of multiple pulses at 3 W and exhibited a pronounced CW component and narrower width $\Delta\lambda_{FWHM} \approx 2 \text{ nm}$ in the single-pulse regime. This was accomplished by starting the oscillator in the multi-pulsing regime and bringing it to the single-pulse regime by reducing the pump power.

The thickness of the plate was further decreased down to 3 mm. KLM was achieved by going to the stability edge and pushing the stage with mirror *R2*. Multiple pulses can be recognized by the strong modulation of the optical spectrum. The decrease of the pump power leads to stable single-pulse operation at 4.5 W output power. There are two noticeable differences in comparison with previous regimes in the presence of strong nonlinearity. First, the spectral bandwidth $\Delta\lambda_{FWHM} \approx 3 \text{ nm}$ is much broader and accordingly pulses are shorter. Second, the difference in output power between the mode-locked and CW regimes becomes more pronounced. This difference $P_{ML}/P_{CW} = 4.5\text{W}/1.5\text{W} = 3$ indicates a large effective modulation depth of the KLM mechanism.

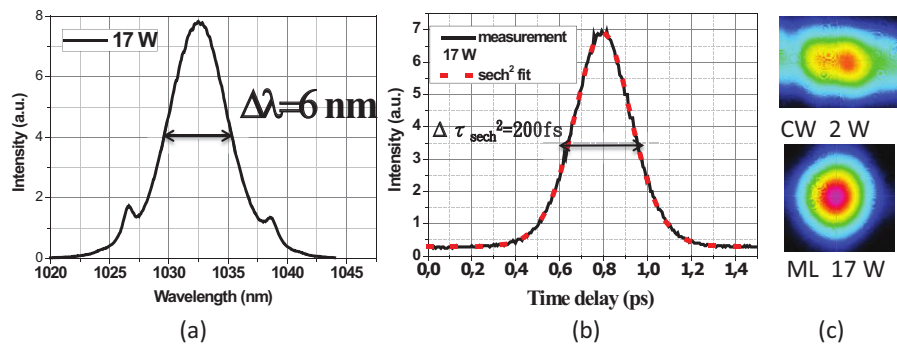


Figure 5. Oscillator characteristics operating with 1-mm-thick fused silica plate as Kerr medium. (a): Optical spectrums at 17 W; (b): Autocorrelation trace at 17 W; (c): Beam profile in the CW and ML regimes.

The best performance was achieved with a 1-mm-thick fused silica plate as Kerr medium. The oscillator was successfully operated with two different output couplers with 5.5% and 14% transmission. With the lower output coupling, we achieved 17 W of average power at 110 W of pump power, which corresponds to an optical-to-optical efficiency of 15%. Under these conditions, we measured a pulse duration of 200 fs (assuming a sech^2 pulse shape) with a spectral width of 6 nm (FWHM) and time-bandwidth product of 0.34 (ideal 0.315); see Fig.5. Kelly sidebands are visible in the spectral wings. As can be seen the spectral bandwidth $\Delta\lambda_{FWHM} \approx 6 \text{ nm}$ approaches the emission-bandwidth limit of Yb:YAG and the difference in output power between the mode-locked and CW regimes is now very pronounced (see Fig. 5(c)). This difference $P_{ML}/P_{CW} = 17\text{W}/2\text{W} = 8$ indicates the large effective modulation depth of the KLM mechanism, which according to the simulations is $\Delta R_{KLM} = 5\%$. With high output coupling, we could achieve stable operation up to pump power levels of 180 W, resulting in an average output power of 45 W, corresponding to 1.1- μJ pulses and 25% optical-to-optical efficiency. The autocorrelation and spectral shapes are shown in Fig.6 with a pulse duration of 270 fs, a spectral width of 4.9 nm (FWHM) and the time-bandwidth product of 0.37 (ideal 0.315). In both operation regimes, the intracavity pulse energy was approximately 8 μJ and the intracavity average power was 320 W. The attempts to reach higher energy led to the onset of multipulsing or CW background. Again, the strong hysteresis behaviour of the oscillator was utilized to start and reach a stable operation regime. At high pump power levels of approximately 150 W for 5.5% OC and 220 W for 14% OC the oscillator self-started in multiple pulses or with CW background; afterwards, the pump power was decreased to bring the oscillator into stable single-pulse operation.

Q-switched mode-locking instabilities used to appear only during the alignment of the oscillator. The suppression of these instabilities is very likely caused by saturation of the KLM self-amplitude modulation.

A small red shift of the spectrum relatively to the gain maximum at 1030 nm could be observed. This shift amounts to 1-2.5 nm and is more pronounced for higher intracavity peak powers. It can be explained by the action of radiation reabsorption in combination with gain saturation and dispersion of the gain medium.^{36,37} Typically, the optimal cavity alignment and mode-locking regime corresponded to a maximal red shift of the spectrum.

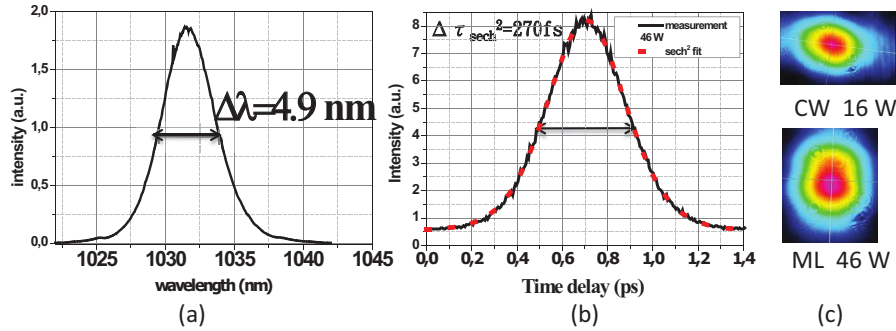


Figure 6. Oscillator characteristics operating with 1-mm-thick fused silica plate and 14% OC. (a): Optical spectra at 46 W; (b): Autocorrelation trace at 46 W; (c): Beam profile in CW and ML regime.

It is worth noting that the cavity in the CW regime is not sensitive to the alignment of such a thin plate as long as its position x relatively to the focus is fixed. The light refraction in the thin plate is weak, thus small misalignment from the Brewster angle due to a plate exchange or due to a shift along the focus is not critical for the overall cavity alignment.

The above-described experiments were carried out with the weak SESAM as a starter for mode-locking. In order to check the influence of a weak SESAM on the oscillator performance, it was replaced (see position M in Fig.3) by an HR mirror. The first experiment was carried out without a hard aperture inside the resonator and KLM was realized due to the soft-aperture on the TD pump spot. This oscillator configuration showed high sensitivity to the position d at the stability edge as well as difficult start-up. Critical sensitivity to the alignment and difficult start-up were decisive factors for not using this configuration for further experiments.

An additional hard-aperture in the form of a pinhole was added into the cavity between the focus and concave mirror $R2$ (see Fig.3). The hard-aperture drastically reduced the alignment sensitivity of the oscillator and simplified the starting procedure. The oscillator could easily be started by pushing mirror $R2$ or self-started at increased pump power levels, as described for weak-SESAM-assisted KLM. In the first experiments a simple 1-mm-thick copper plate with a drilled hole >2 mm in diameter in it was used as a hard-aperture. Due to the high intracavity power >300 W it quickly warmed up and caused an oscillator drift. In order to eliminate this issue a water-cooled monolithic copper aperture (Fig.7(c)) was recently designed and used in later experiments. This water-cooled aperture does not cause pronounced drift of the oscillator, but it also hardly tolerates such oscillator drifts due to the thermal effects in the intracavity optics. Thus, several alignments may be necessary due to the oscillator warm-up. Once aligned, the oscillator keeps running stably for the whole day. With the low output coupling of 5.5% we achieved 15 W of average power. Under these conditions, we measured a pulse duration of 190 fs (assuming a sech^2 pulse shape) with a spectral width of 6.5 nm (FWHM) in Fig.7(a), which is 10% broader than that reported for the SESAM-assisted case. This pulse shortening by 10% is due to the combined action of the soft and hard apertures with somewhat higher effective modulation depth. This argument can also be checked by the absence of Kelly sidebands in the optical spectrum in Fig.7(a).

A test experiment was made by exchanging the 1-mm-thick plate for a 0.5-mm-thick plate. The alignment relatively to the beam focus became more critical. The oscillator was not self-starting as described before, but slight mirror perturbation was sufficient to initiate KLM. The regime showed single-pulse operation with characteristics similar to the case with the 1-mm plate at somewhat higher output power.

3.2 Damage to HD mirrors and Kerr medium

Unlike in the experiments with a pure SESAM mode-locked oscillator, damage of the weak overcoated SESAM was not observed. There are two reasons for this: first, the field penetration-depth into the SESAM structure

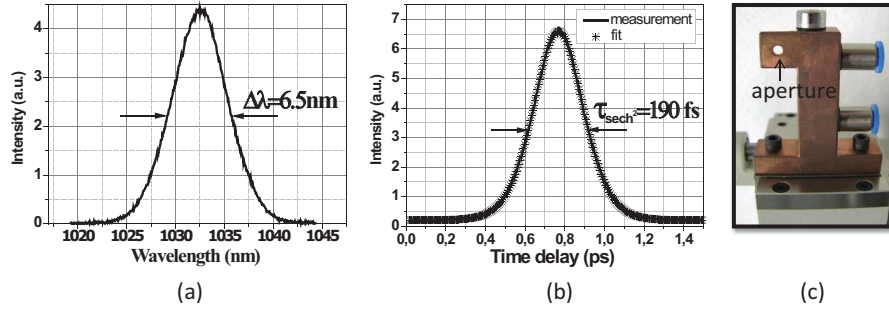


Figure 7. Oscillator characteristics operating with 1-mm-thick fused silica plate, 5.5% OC and hard-aperture. (a): Optical spectrums at 15 W; (b): Autocorrelation trace at 15 W; (c): Water-cooled hard-aperture.

is by a factor 9 less than for the usual SESAM with no dielectric coating; second, the beam on the end mirror is enlarged near the stability edge and consequently reduces the peak intensity on it. However, damage to the HD mirrors and the Kerr medium was observed. This damage was only observed during oscillator start-up and alignment. It was mostly caused both by the non-optimal position x of the Kerr medium relatively to the focus and by moving the oscillator too close to the stability edge via changing the distance d . It was noticed that HD mirrors located closer to the output coupler and that those with higher GDD values were most susceptible to damage. The beam diameter shrinks near the stability edge in the part of the oscillator close to the output coupler and makes the optics in this part most susceptible to damage during the oscillator start-up. As long as the oscillator is optimally aligned it can be started and run with no damage to the optical elements.

3.3 Energy scaling of KLM

KLM as realized in our work allows energy/power scaling. The average power scaling is supported by the TD concept and the cavity calculations show that spot sizes over 5 mm on the TD are feasible. Energy scaling can be performed by increasing the mode size inside the Kerr medium in proportion to the increase of the intracavity energy. This procedure would keep the peak intensity and self-focusing parameters in the Kerr medium constant. This can be accomplished in turn by exchanging the mirrors $R1$ and $R2$ for new ones with larger radii of curvature. The mirrors $R1$, $R2$ separated by the distance d can be considered as a telescopic 4f arrangement in first approximation. Consequently, exchanging the mirrors will not influence the beam parameters on other critical cavity elements such as the TD. Further optimization of KLM can be accomplished by changing the thickness of the Kerr medium.

The theoretical analysis based on the variational approximation³⁸ suggests the following laws for energy scaling in the anomalous dispersion KLM regime under the condition of $\gamma/\Omega^2 |\beta| \kappa \gg 1$ (γ is the net-SPM coefficient, Ω is the gain bandwidth multiplied by square root of the oscillator net-loss; β is the net-GDD coefficient; κ is the inverse power coefficient characterizing the KLM mechanism, e.g. effective gain increase with power for soft-aperture KLM or effective loss decrease with power for hard-aperture KLM) :

$$E \approx \sqrt{\frac{20\mu |\beta|}{\kappa\gamma}}, \quad (1)$$

for soft aperture KLM, and

$$E \approx \frac{3.5\Omega |\beta| \sqrt{\mu}}{\gamma}, \quad (2)$$

for hard aperture KLM (here μ is the effective modulation depth of the KLM mechanism).

Since $\kappa \propto \gamma$ due to the inherent connection between KLM and SPM, one may conclude that hard aperture KLM provides better energy scalability with GDD and such the scalability improves with gainband broadening. The SPM reduction is able to improve the scalability as well. But one has to keep in mind that such a reduction

makes the start-up process more difficult; thus there exists an some optimal value for SPM for in a given configuration of the laser.

4. OSCILLATOR STABILITY IN THE ANOMALOUS DISPERSION REGIME

4.1 Beam pointing

The oscillator is operating in the stability zone II³⁹ with large mode sizes. Despite this, the laser shows excellent beam pointing stability with $<10 \mu\text{rad}$ r.m.s. deviation, as can be derived from the measurements in Fig.8(b). Figure 8(a) shows the beam pointing drift during oscillator warm-up, which takes 10-30 minutes. Beam pointing

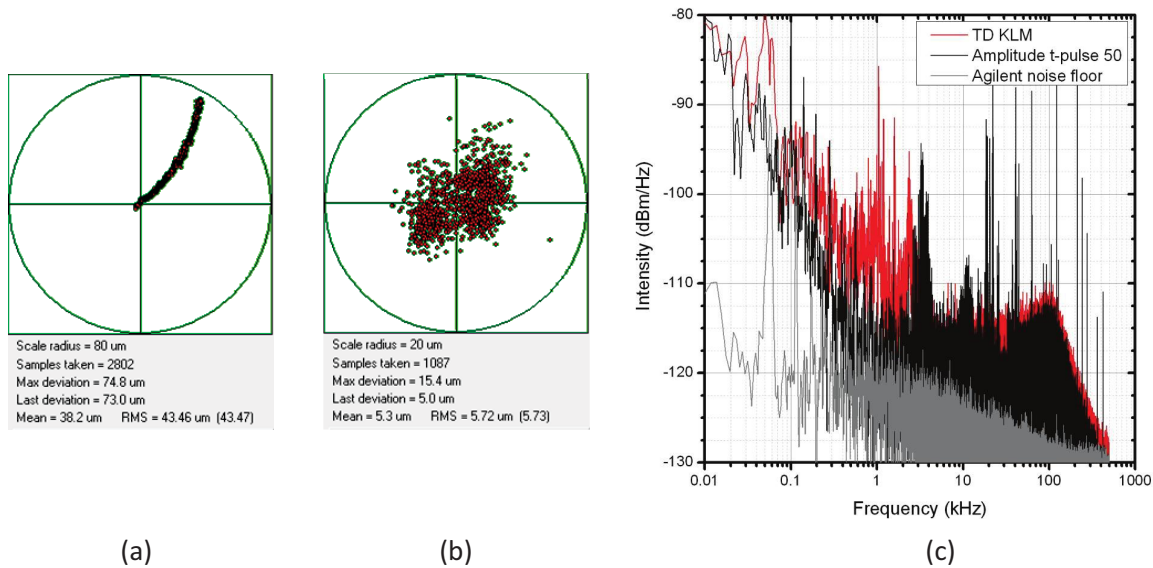


Figure 8. Beam pointing fluctuations of the mode-locked oscillator at 1 m distance from the output coupler (measured with WinCam beam profiler). (a): Beam pointing drift during oscillator warm-up; (b): Beam pointing fluctuations after oscillator warm-up; (c): Power spectral density (PSD) of intensity noise from the free-running Yb:YAG TD KLM oscillator (red curve), from the commercial oscillator Amplitude t-pulse 50 (black curve) and the noise floor of the Agilent spectrum analyzer (gray curve).

fluctuations correspond to the level of commercial Ti:Sa oscillators, and so no active stabilization schemes are needed for further experiments with this laser. Many research applications such as CEP stabilization,⁴⁰ spectrum broadening,⁴¹ white light generation, repetition rate synchronization⁴² and seeding of enhancement cavities³ call for unprecedented power stability of the oscillator, specifically on a short time scale. All these experiments utilize nonlinear phenomena, thus any small intensity fluctuations of a driving field can be transferred to the amplitude and phase noise of the output signal. The oscillator intensity noise is typically caused by fluctuations of the pump diodes and by external mechanical noise. The power spectral density of the intensity fluctuations is shown in Fig.8(c). The main intensity noise lies within the 5 kHz bandwidth and has a small relaxation oscillation spike near 1 kHz. Corresponding r.m.s. fluctuations are below 0.3%. Intensity noise is compared to the commercial Yb-oscillator Amplitude t-pulse 50 (black curve in Fig.8(c)), which has 20 times lower pulse energy and average power. Intensity fluctuations of our TD KLM system are comparable to those of commercial oscillators.

It is difficult to give an adequate comparison between the intensity noise of the pure SESAM mode-locked TD oscillator³⁰ and the KLM TD oscillator as the first one was mode-locked at 3 times higher intracavity pulse energies than the former, but with similar intracavity peak powers of 40 MW. Generally the SESAM mode-locked oscillator had a stronger tendency to Q-switched mode-locking, which was not observed in the KLM oscillator. The simplest way of characterizing intensity fluctuations is to detect the repetition rate frequency with an RF spectrum analyzer. As shown in Fig.9, the sidebands in the case of the SESAM mode-locked oscillator are suppressed by 60 dBm and sidebands of the KLM oscillator are suppressed by 70-75 dBm. It is worth noting that suppression of the sidebands by 40 dB was reported for a SESAM-ML active multi-pass oscillator.^{6,43} This shows a remarkable superiority of KLM over SESAM mode-locking.

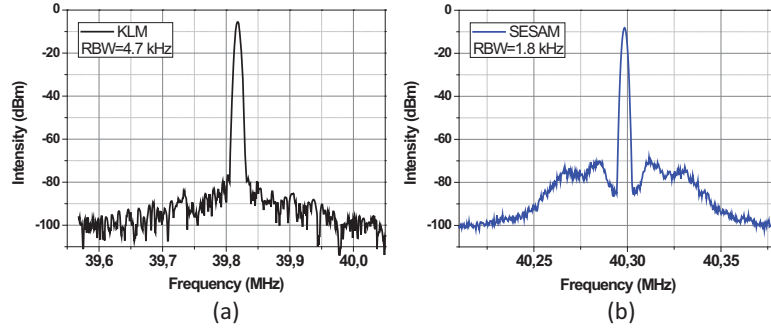


Figure 9. The radio frequency spectra showing the repetition rate beat signal at ~ 40 MHz. (a): KLM Yb:YAG TD oscillator; (b): SESAM mode-locked Yb:YAG TD oscillator.

4.2 Sensitivity to back reflections

Typically, back reflections disturb the oscillator operation and can cause strong fluctuations or interrupt mode-locking. Measures should be taken to avoid back reflections from all intracavity elements, and so TD and OC should be wedged. Moreover, a Faraday isolator may be necessary to prevent back reflections from the experimental setup outside the cavity. The sensitivity of the oscillator to back reflections was tested by placing a plane-parallel output coupler with 2% transmission having an AR coating $< 0.1\%$ instead of the wedged one. The oscillator could easily be mode-locked at 6 W output power; no pulse train modulation was noticed. Moreover, the mode-locking could not be disturbed even by placing a HR mirror after the output coupler and reflecting back all of the 6 W output power. Further experiments with spectrum broadening in a fibre and CE phase characterization were performed without the Faraday isolator and with no influence on the oscillator performance. The influence of back reflections on the self-starting oscillator behaviour⁴⁴ was not studied.

5. KERR-LENS MODE-LOCKED YB:YAG THIN-DISK CHIRPED-PULSE OSCILLATOR

The regime of normal intracavity GDD has already demonstrated its potential for energy scaling of long-cavity Ti:Sa oscillators,⁴⁵ reaching pulse energies of > 500 nJ¹⁰ and more recently > 650 nJ in commercial systems.¹¹ This approach has also been applied to SESAM mode-locked Yb:KYW and Yb:KLuW bulk⁴⁶ and TD⁴⁷ oscillators allowing a substantial increase of the intracavity pulse energy. Nevertheless, while constituting the standard operation regime of femtosecond fibre oscillators,⁴⁸ normal GDD is still an exception to the rule in bulk solid-state oscillators. As a follow-up of our work on the Yb:YAG KLM TD oscillator in the anomalous GDD regime, here the operation of such a system is described in the regime of normal intracavity GDD. The experimental setup is practically the same as the one in Fig.3(a) for the case of the anomalous GDD.

At first, pure KLM was tried by using a hard-aperture. However, all attempts to start this mode of operation proved unsuccessful (as opposed to the system operated with anomalous GDD, where hard-aperture KLM could be readily started. Therefore, the results reported here were achieved with soft-aperture KLM and with the assistance of a weak SESAM employed merely for self-starting mode-locking.

Theoretical analysis based on the variational approximation³⁸ predicts the following energy scaling law for the chirped sech-shaped pulses in the normal dispersion soft-aperture KLM regime:

$$E \approx \frac{34\Omega\beta\sqrt{\mu}}{\kappa}, \quad (3)$$

while for the flat-top-shaped pulses the energy scalability is ideal when $\beta \rightarrow 1.5\gamma/\kappa\Omega^2$ (so-called dissipative soliton resonance;⁴⁹ the latter condition is obtained on the basis of the adiabatic theory³⁸).

The normal intracavity GDD regime has several advantages over the anomalous one. The peak power inside the oscillator is drastically reduced owing to a large pulse chirp and remains constant with energy scaling. As a result, the GDD needed to stabilize a pulse is approximately an order of magnitude less than in the anomalous GDD regime. This means that an energy scaling-scheme with normal GDD is superior to one employing the anomalous GDD (compare Eqs. (1) and (3)). Moreover, the normal dispersion regime can provide an ideal energy scalability via the increase of average power when scaling of the GDD is not required at all. Further the normal GDD allows shorter pulses after compression down to the Fourier limit. Indeed, a solitonic pulse duration τ scales with the anomalous GDD in the soft-aperture regime as

$$\tau \approx 0.45 \sqrt{\frac{\kappa_s \beta}{\gamma \mu}}. \quad (4)$$

This expression corresponds to the width of chirped sech-shaped pulses after compression. In the case of ideal energy scaling, however, the minimal pulse width in the normal GDD regime with the soft-aperture KLM does not depend on GDD and approaches the value of $\tau \rightarrow 0.3/\Omega\sqrt{\mu}$ which is defined only by gain-bandwidth, oscillator net-loss and modulation depth.

5.1 Oscillator start-up

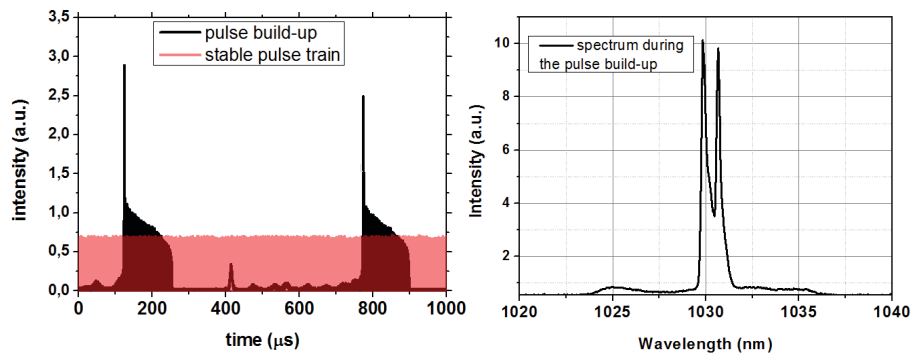


Figure 10. Oscillator self-starting behaviour. (a): Pulse train during build-up (black) and mode-locked pulse train (red); (b): Spectrum corresponding to the pulse build-up.

The benefits of the normal GDD regime come at the expense of a more challenging start-up behaviour of the mode-locking process. In practice pulse formation with normal GDD can only be initiated within a limited parameter window (of the SPM and GDD values). In contrast to anomalous-regime-KLM which tends to start in the multiple-pulse regime, normal intracavity GDD tends to prefer the formation of a single pulse in the cavity. As compared with our KLM disk laser operated originally with a net intracavity GDD of -22000 fs^2 , a normal GDD nearly an order of magnitude smaller was chosen while leaving other parameters of the cavity unchanged. The round-trip GDD of $+3500 \text{ fs}^2$ was introduced by 4 bounces on dispersive mirrors. This modification of the cavity did not allow mode-locking. Therefore, subsequent increase of SPM inside the cavity was performed by replacing the 1-mm-thick fused-silica nonlinear medium with one having a thickness of a quarter of an inch (6.4 mm).

The pulse build-up process is rather hard and starts most likely from Q-switching. This Q-switching often resulted in white light generation and occasionally damaged the Kerr medium but never damaged any other optics in the cavity. The transit situation, when the oscillator is close to the optimal point and tries to build up a pulse train, is shown in Fig.10. A small pump power increase leads to a stable pulse train, depicted by the red curve in Fig.10(a). The peak intensity is at least six times higher during the oscillator start-up than for the stable situation (compare black and red traces). The optical spectrum corresponding to the start-up situation is shown in Fig.10(b). It exhibits both a CW component and small broad pedestal corresponding to the mode-locked pulse train. The experiments were carried out with output couplers of 5.5% and 10% transmission and 6.4- and 9.5-mm-thick fused-silica Kerr media. Generally, the tendency for softer self-start and alignment flexibility was observed for the case of the 5.5% OC and 6.4-mm-thick Kerr plate.

5.2 Results

In the configuration with an output coupling of 5.5%, 17 W of average power at 150 W of pump power was achieved, which corresponds to an optical-to-optical efficiency of 11%. Under these conditions, a pulse duration of ≈ 2 ps (assuming a sech^2 pulse shape, Fig.12(a)) with a full spectral width of over 20 nm (see red spectrum in Fig.11) was measured. The calculated Fourier limit is 150 fs. The pulses were compressed externally in an all-dispersive mirror compressor introducing $-60,000 \text{ fs}^2$ GDD at 20 bounces.³⁴ The resulting pulse duration after the compressor is 190 fs full-width at half-maximum (assuming a sech^2 pulse profile) with 11 W throughput (Fig.12(b)). The relatively high loss of 40% in the compressor is caused by clipping the beam on the mirrors and is related to the limited amount of mirrors. The pedestal in the autocorrelation trace (Fig.12(b)) may be caused

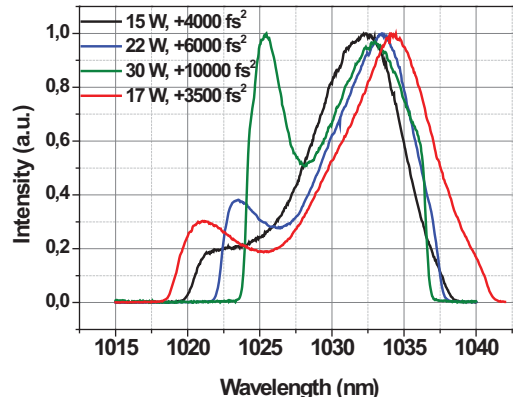


Figure 11. The spectra at different output power levels. The red spectrum was measured at 17 W of output power, a 5.5% output coupler and a 6.4-mm-thick Kerr plate. The other spectra were measured with 10% output coupler and 9.5-mm-thick Kerr plate.

by the high-dispersive mirrors, which were designed for the range 1030 ± 10 nm and could be slightly shifted in the central wavelength because of coating deposition errors.³⁴ Depending on the mode-locking parameters, the spectrum can exhibit strong non-linear chirp at the edges, a common feature of the normal dispersion regime. The autocorrelation with pedestal may be due to an uncompensated non-linear chirp.⁵⁰ The issue of optimal compression corresponding to the maximally “flat” chirp⁵¹ was beyond the scope of this work. The spectral

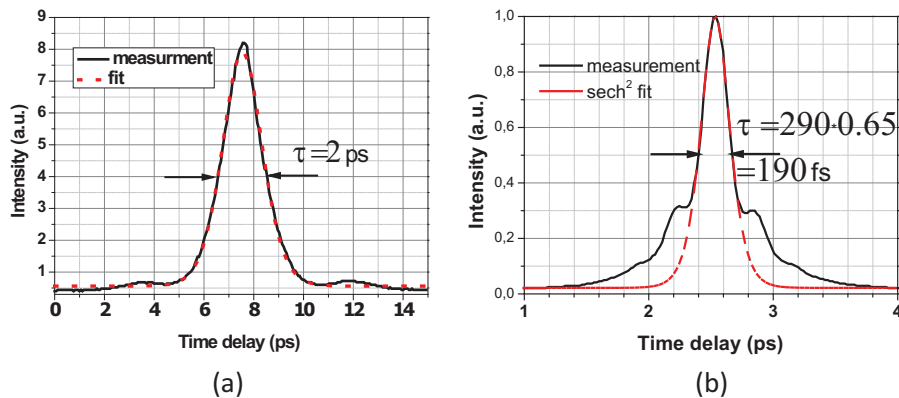


Figure 12. The autocorrelation measurements before compressor (a) and after compressor (b).

shapes in Fig.11 have relatively smooth edges as a result of the narrow gain-bandwidth and the relatively large net loss^{10,38} and become more truncated with the growth of the GDD. Also, there is an asymmetry of the spectra relatively to the emission bandwidth maximum at ~ 1030 nm. This can be explained by a similarly asymmetric shape of the Yb:YAG gain and the high-order dispersion induced by phase change in such a narrow-band gain medium.⁵²

After the oscillator self-started it was slightly realigned to operate closer to the stability edge by means of increasing the distance d (see Fig.3(a)) and proportionally the pump power. This optimization procedure typically provided an increase of the average power by 30%; see blue, olive and black spectra in Fig.11, measured with 10% output coupler transmission and 9.5-mm-thick Kerr plate. An extreme case is the red spectrum in Fig.11, measured with 5.5% output coupling and a 6.4-mm-thick Kerr plate. In this case the output power could be increased by 50%, from 12 W to 17 W. A slight increase of the pump power by 3-5% with all other parameters fixed resulted in a tendency to instabilities and strong Q-switching, similar to that in the build-up process (see Fig.10(a)). Decrease of the pump power by the same amount always brought the laser back into the stable regime (see Fig.10(b)). This was characterized by typical peak-to-peak amplitude fluctuations of <3% within the 1-minute measurement time, a value significantly higher than that for the negative GDD regime.

As predicted in Ref.,³⁸ a normal GDD regime in combination with soft-aperture KLM can allow powerful energy scaling without the need for a substantial GDD increase and comprising bandwidth. Nevertheless, we found experimentally that the energy growth increasingly impedes the ability of the laser to self-start and requires an increase of the GDD level for self-starting KLM. Such a GDD growth required for self-starting results in spectral narrowing (Fig.11). This behaviour is similar to the one reported in.⁵³ The oscillator could substantially benefit from the ability to tune the GDD inside the cavity and use this 'knob' to implement a hysteresis in the energy vs GDD coordinates. This was realized by means of two prisms.⁵⁴ Our attempts to initiate mode-locking at an increased GDD level $>+10000$ fs² were not successful. Further power scaling of the oscillator with normal GDD was limited by the inability to start mode-locking.

5.3 Summary

Even though the difficult mode-locking initiation can be explained qualitatively by the long chirped pulses, being especially critical for KLM, the details and theoretical investigation of the starting mechanism remains one of the most intriguing and non-investigated issues for energy-scalable oscillators. This work provides strong motivation for theoretical research on the starting mechanism, specifically in the normal GDD regime. 0.4- μ J pulses with an average power of 17 W and a pulse duration of 190 fs were demonstrated. This result is realized with nearly an order smaller GDD compared with the regime of anomalous GDD. Power scaling with GDD and output coupling up to 30 W demonstrated, however, approaching GDD levels similar to the negative dispersion regime (Fig.11). Inability to start the oscillator at increased GDD levels was found to be the limiting factor in further energy scaling. An additional starting mechanism such as regenerative mode-locking²⁸ or SESAM¹³ with an increased modulation depth offers the potential for scaling the pulse energy and the power of KLM disk lasers to unprecedented values.

6. CONCLUSION

This paper describes the experimental steps in the first realization of KLM in the TD oscillators, motivated by the limitations of SESAM mode-locking. The experimental results of the oscillator operating with 0.5-, 1-, 3-, 6-mm-thick fused silica as Kerr medium are presented. The best performance was reached with the 1-mm-thick Kerr plate and a total GDD of -22000 fs². The oscillator was successfully operated with two different output couplers of 5.5% and 14% transmission. With 5.5% transmission 200 fs pulse duration and 0.4 μ J pulse energy with 17 W of average power at 15% optical-to-optical efficiency was achieved. With higher output coupling the parameters were 250 fs, 1.1 μ J, 45 W and 25% efficiency. These results were obtained with a weak SESAM having both negligible modulation depth $\Delta R < 0.1\%$ and thermal effects. The chip was developed in the frame of this work. Pure hard-aperture KLM was also realized with similar parameters and a somewhat shorter pulse duration of 190 fs. Intensity fluctuations of the oscillator are below 0.3% r.m.s. The laser shows excellent beam pointing stability with <10 μ rad and is insensitive to back reflections. This oscillator configuration was also operated in the normal dispersion regime with the weak SESAM as a starter. The average power of 17 W and pulse duration of 1.7 ps with a full spectral width of over 20 nm could be reached at an output-coupling transmission of 5.5%. The pulses were externally compressed down to 190 fs. These parameters were obtained at nearly an order of magnitude lower GDD in comparison with the negative dispersion regime. It was found that the main factor preventing further energy scaling is an inability of the laser to self-start.

REFERENCES

1. F. Krausz and M. Ivanov, "Attosecond physics," *Rev. Mod. Phys.* **81**, pp. 163–234, 2009.
2. C. Gohle, T. U. M. Herrmann, J. Rauschenberger, R. Holzwarth, H. A. Schuessler, F. Krausz, and T. W. Hänsch, "A frequency comb in the extreme ultraviolet," *Nature* **436**, pp. 234–237, 2005.
3. A. Cingöz, D. C. Yost, T. K. Allison, A. Ruehl, M. E. Fermann, I. Hartl, and J. Ye, "Direct frequency comb spectroscopy in the extreme ultraviolet," *Nature* **482**, pp. 68–71, 2012.
4. P. Baum and A. H. Zewail, "Attosecond electron pulses for 4d diffraction and microscopy," *Proceedings of the National Academy of Sciences* **104**, pp. 18409–18414, 2007.
5. I. Pupeza, T. Eidam, J. Rauschenberger, B. Bernhardt, A. Ozawa, E. Fill, A. Apolonski, T. Udem, J. Limpert, Z. A. Alahmed, A. M. Azzeer, A. Tünnermann, T. W. Hänsch, and F. Krausz, "Power scaling of a high-repetition-rate enhancement cavity," *Opt. Lett.* **35**(12), pp. 2052–2054, 2010.
6. D. Bauer, I. Zawischa, D. H. Sutter, A. Killi, and T. Dekorsy, "Mode-locked Yb:YAG thin-disk oscillator with 41 μ J pulse energy at 145 W average infrared power and high power frequency conversion," *Opt. Express* **20**, p. 9698, 2012.
7. C. J. Saraceno, F. Emaury, O. H. Heckl, C. R. E. Baer, M. Hoffmann, C. Schriber, M. Golling, T. Südmeyer, and U. Keller, "275 W average output power from a femtosecond thin disk oscillator operated in a vacuum environment," *Opt. Express* **20**, pp. 23535–23541, 2012.
8. O. Pronin, J. Brons, C. Grasse, V. Pervak, G. Boehm, M.-C. Amann, V. L. Kalashnikov, A. Apolonski, and F. Krausz, "High-power 200 fs Kerr-lens mode-locked Yb:YAG thin-disk oscillator," *Opt. Lett.* **36**(24), pp. 4746–4748, 2011.
9. E. Seres, J. Seres, and C. Spielmann, "Extreme ultraviolet light source based on intracavity high harmonic generation in a mode locked Ti:sapphire oscillator with 9.4 MHz repetition rate," *Opt. Express* **20**(6), pp. 6185–6190, 2012.
10. S. Naumov, A. Fernandez, R. Graf, P. Dombi, F. Krausz, and A. Apolonski, "Approaching the microjoule frontier with femtosecond laser oscillators," *New J. Phys.* (1), p. 216, 2005.
11. <http://www.femtolasers.com/Oscillator.50.0.html>.
12. A. Stingl, M. Lenzner, C. Spielmann, F. Krausz, and R. Szipöcs, "Sub-10-fs mirror-dispersion-controlled Ti:sapphire laser," *Opt. Lett.* **20**(6), pp. 602–604, 1995.
13. D. H. Sutter, G. Steinmeyer, L. Gallmann, N. Matuschek, F. Morier-Genoud, U. Keller, V. Scheuer, G. Angelow, and T. Tschudi, "Semiconductor saturable-absorber mirror assisted Kerr-lens mode-locked Ti:sapphire laser producing pulses in the two-cycle regime," *Opt. Lett.* **24**(9), pp. 631–633, 1999.
14. A. Greborio, A. Guandalini, and J. A. der Au, "Sub-100 fs pulses with 12.5-W from Yb:CALGO based oscillators," *Solid State Lasers XXI: Technology and Devices* **8235**(1), p. 823511, SPIE, 2012.
15. T. Eidam, S. Hanf, E. Seise, T. V. Andersen, T. Gabler, C. Wirth, T. Schreiber, J. Limpert, and A. Tünnermann, "Femtosecond fiber CPA system emitting 830 W average output power," *Opt. Lett.* **35**(2), pp. 94–96, 2010.
16. P. Russbueldt, T. Mans, J. Weitenberg, H. D. Hoffmann, and R. Poprawe, "Compact diode-pumped 1.1 kW Yb:YAG innoslab femtosecond amplifier," *Opt. Lett.* **35**(24), pp. 4169–4171, 2010.
17. U. Keller, "Recent developments in compact ultrafast lasers," *Nature* **424**, pp. 831–838, 2003.
18. R. Paschotta and U. Keller, "Ever higher power from mode-locked lasers," *Opt. Photon. News* **14**(5), pp. 50–54, 2003.
19. U. Keller, "Ultrafast solid-state laser oscillators: a success story for the last 20 years with no end in sight," *Appl. Phys. B* **100**, pp. 15–28, 2010.
20. M. Piché, "Beam reshaping and self-mode-locking in nonlinear laser resonators," *Opt. Commun.* **86**(2), pp. 156–160, 1991.
21. G. Cerullo, S. D. Silvestri, and V. Magni, "Self-starting Kerr-lens mode locking of a Ti:sapphire laser," *Opt. Lett.* **19**(14), pp. 1040–1042, 1994.
22. D. Huang, M. Ulman, L. H. Acioli, H. A. Haus, and J. G. Fujimoto, "Self-focusing-induced saturable loss for laser mode locking," *Opt. Lett.* **17**(7), pp. 511–513, 1992.
23. V. L. Kalashnikov, V. P. Kalosha, I. G. Poloyko, and V. P. Mikhailov, "Optimal resonators for self-mode locking of continuous-wave solid-state lasers," *J. Opt. Soc. Am. B* **14**(4), pp. 964–969, 1997.

24. E. Wintner, E. Sorokin, and I. Sorokina, "Laser system for producing ultra-short light pulses." US Patent 6363090B1, 2002.
25. B. Henrich and R. Beigang, "Self-starting Kerr-lens mode locking of a Nd:YAG-laser," *Opt. Commun.* **135**, pp. 300 – 304, 1997.
26. G. P. A. Malcolm and A. I. Ferguson, "Self-mode locking of a diode-pumped Nd:YLF laser," *Opt. Lett.* **16**(24), pp. 1967–1969, 1991.
27. Y. M. Liu, K. W. Sun, P. R. Prucnal, and S. A. Lyon, "Simple method to start and maintain self-mode-locking of a Ti:sapphire laser," *Opt. Lett.* **17**(17), pp. 1219–1221, 1992.
28. L. Turi and F. Krausz, "Amplitude modulation mode locking of lasers by regenerative feedback," *Appl. Phys. Lett.* **58**(8), pp. 810–812, 1991.
29. I. P. Bilinsky, R. P. Prasankumar, and J. G. Fujimoto, "Self-starting mode locking and Kerr-lens mode locking of a Ti:Al₂O₃ laser by use of semiconductor-doped glass structures," *J. Opt. Soc. Am. B* **16**, pp. 546–549, Apr 1999.
30. O. Pronin, V. Kalashnikov, V. Pervak, C. Teisset, M. Larionov, J. Rauschenberger, A. Apolonski, E. Fill, and F. Krausz, "Scalability of mode-locked thin-disk oscillators: issues and scenarios of destabilization," in *CLEO/Europe and EQEC 2011 Conference Digest, CLEO/Europe and EQEC 2011 Conference Digest*, p. CA11.5, Optical Society of America, 2011.
31. C. J. Saraceno, C. Schriber, M. Mangold, M. Hoffmann, O. H. Heckl, C. R. E. Baer, M. Golling, T. Südmeyer, and U. Keller, "Sesams for high-power oscillators: design guidelines and damage thresholds," *IEEE J. Quantum Electron.* **18**, pp. 29–41, 2012.
32. S. Uemura and K. Torizuka, "Sub-40-fs pulses from a diode-pumped Kerr-lens mode-locked Yb-doped yttrium aluminum garnet laser," *Jap. J. Appl. Phys.* **50**(1), p. 010201, 2011.
33. C. Hönninger, R. Paschotta, M. Graf, F. Morier-Genoud, G. Zhang, M. Moser, S. Biswal, J. Nees, A. Braun, G. Mourou, I. Johannsen, A. Giesen, W. Seeber, and U. Keller, "Ultrafast ytterbium-doped bulk lasers and laser amplifiers," *Appl. Phys. B* **69**, pp. 3–17, 1999.
34. V. Pervak, O. Pronin, O. Razskazovskaya, J. Brons, I. B. Angelov, M. K. Trubetskov, A. V. Tikhonravov, and F. Krausz, "High-dispersive mirrors for high power applications," *Opt. Express* **20**(4), pp. 4503–4508, 2012.
35. R. Adair, L. L. Chase, and S. A. Payne, "Nonlinear refractive index of optical crystals," *Phys. Rev. B* **39**, pp. 3337–3350, 1989.
36. V. L. Kalashnikov, E. Sorokin, and I. T. Sorokina, "Mechanisms of spectral shift in ultrashort-pulse laser oscillators," *J. Opt. Soc. Am. B* **18**(11), pp. 1732–1741, 2001.
37. V. L. Kalashnikov, E. Sorokin, S. Naumov, and I. T. Sorokina, "Spectral properties of the Kerr-lens mode-locked Cr⁴⁺: YAG laser," *J. Opt. Soc. Am. B* **20**(10), pp. 2084–2092, 2003.
38. V.L.Kalashnikov, *Solid state lasers*, ch. Chirped-Pulse Oscillators: Route to the Energy-Scalable Femtosecond Pulses, pp. 145–184. InTech, 2012.
39. V. Magni, "Multielement stable resonators containing a variable lens," *J. Opt. Soc. Am. A* **4**(10), pp. 1962–1969, 1987.
40. S. A. Meyer, J. A. Squier, and S. A. Diddams, "Diode-pumped Yb:KYW femtosecond laser frequency comb with stabilized carrier-envelope offset frequency," *Eur. Phys. J. D* **48**(1), pp. 19–26, 2008.
41. T. Ganz, V. Pervak, A. Apolonski, and P. Baum, "16 fs, 350 nJ pulses at 5 MHz repetition rate delivered by chirped pulse compression in fibers," *Opt. Lett.* **36**(7), pp. 1107–1109, 2011.
42. H. Fattahi, C. Y. Teisset, O. Pronin, A. Sugita, R. Graf, V. Pervak, X. Gu, T. Metzger, Z. Major, F. Krausz, and A. Apolonski, "Pump-seed synchronization for MHz repetition rate, high-power optical parametric chirped pulse amplification," *Opt. Express* **20**(9), pp. 9833–9840, 2012.
43. J. Neuhaus, D. Bauer, J. Zhang, A. Killi, J. Kleinbauer, M. Kumkar, S. Weiler, M. Guina, D. H. Sutter, and T. Dekorsy, "Subpicosecond thin-disk laser oscillator with pulse energies of up to 25.9 microjoules by use of an active multipass geometry," *Opt. Express* **16**(25), pp. 20530–20539, 2008.
44. K. Tamura, J. Jacobson, E. P. Ippen, H. A. Haus, and J. G. Fujimoto, "Unidirectional ring resonators for self-starting passively mode-locked lasers," *Opt. Lett.* **18**(3), pp. 220–222, 1993.

45. S. H. Cho, F. X. Kärtner, U. Morgner, E. P. Ippen, J. G. Fujimoto, J. Cunningham, and W. H. Knox, "Generation of 90-nJ pulses with a 4-MHz repetition-rate Kerr-lens mode-locked Ti:Al₂O₃ laser operating with net positive and negative intracavity dispersion," *Opt. Lett.* **26**(8), pp. 560–562, 2001.
46. G. Palmer, M. Emons, M. Siegel, A. Steinmann, M. Schultze, M. Lederer, and U. Morgner, "Passively mode-locked and cavity-dumped Yb:KY(WO₄)₂ oscillator with positive dispersion," *Opt. Express* **15**(24), pp. 16017–16021, 2007.
47. G. Palmer, M. Schultze, M. Siegel, M. Emons, U. Bünting, and U. Morgner, "Passively mode-locked Yb:KLu(WO₄)₂ thin-disk oscillator operated in the positive and negative dispersion regime," *Opt. Lett.* **33**(14), pp. 1608–1610, 2008.
48. F. Wise, A. Chong, and W. Renninger, "High-energy femtosecond fiber lasers based on pulse propagation at normal dispersion," *Laser & Photon. Rev.* **2**(1-2), pp. 58–73, 2008.
49. W. Chang, A. Ankiewicz, J. M. Soto-Crespo, and N. Akhmediev, "Dissipative soliton resonances," *Phys. Rev. A* **78**, p. 023830, 2008.
50. V. Kalashnikov, E. Podivilov, A. Chernykh, S. Naumov, A. Fernandez, R. Graf, and A. Apolonski, "Approaching the microjoule frontier with femtosecond laser oscillators," *New J. Phys.* (1), p. 217, 2005.
51. E. Podivilov and V. L. Kalashnikov, "Heavily-chirped solitary pulses in the normal dispersion region: new solutions of the cubic-quintic complex ginzburg-landau equation," *JETP Letters* **82**, pp. 467–471, 2005.
52. R. Paschotta, R. Häring, A. Garnache, S. Hoogland, A. Tropper, and U. Keller, "Soliton-like pulse-shaping mechanism in passively mode-locked surface-emitting semiconductor lasers," *Appl. Phys. B* **75**, pp. 445–451, 2002.
53. A. Fernandez, *Chirped-Pulse Oscillators: Generating Microjoule Femtosecond Pulses at Megahertz Repetition Rate*. PhD thesis, LMU München, 2007.
54. A. Fernandez, T. Fuji, A. Poppe, A. Fürbach, F. Krausz, and A. Apolonski, "Chirped-pulse oscillators: a route to high-power femtosecond pulses without external amplification," *Opt. Lett.* **29**(12), pp. 1366–1368, 2004.